Supplemental Information for:

Mechanism-informed refinement reveals altered substrate-binding mode for catalytically competent nitroreductase

Warintra Pitsawong[1,2], Chad A. Haynes[3,4], Ronald L. Koder, Jr.[1,5], David W. Rodgers[3*] & Anne-Frances Miller[1,3*]

[1] Department of Chemistry, University of Kentucky, 505 Rose Street, Lexington, KY, 40506-0055.
[2]Currently: Dept. Biochemistry, Brandeis University, Waltham MA,
[3]Department of Molecular and Cellular Biochemistry and Center for Structural Biology, University of Kentucky, Lexington, KY,
[4]Currently: Booz Allen Hamilton, Washington, DC 20024,
[5]Currently: Dept. Physics, The City College of New York, NY NY,
*Corresponding Authors

Contents

Supplemental Figures

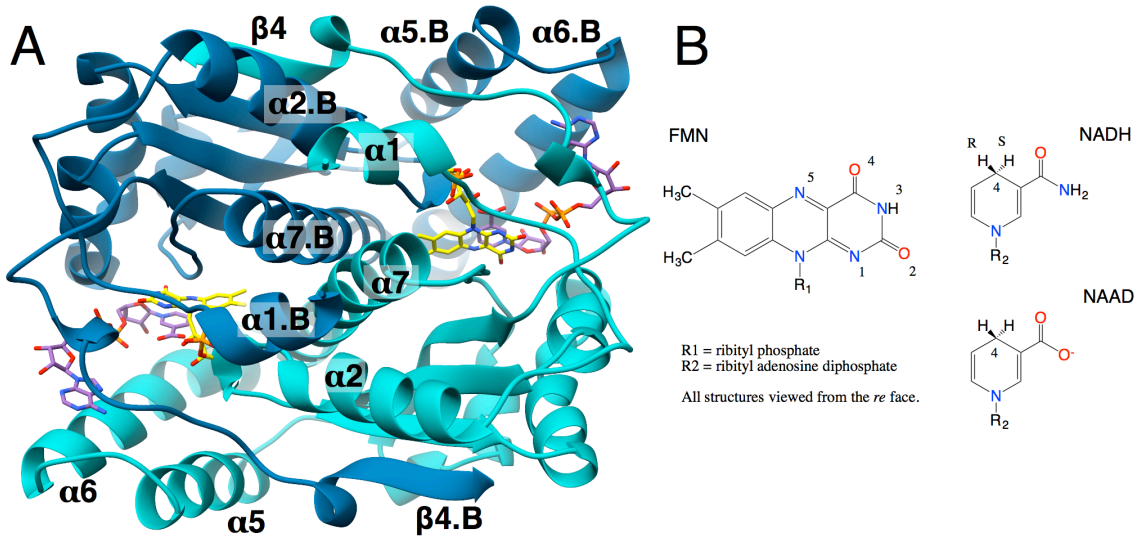

Supplemental Figure S1 related to figures 2 and 6. a: Ribbon depiction of structure of oxidized NR with bound NAAD substrate analog. The flavin (yellow carbons) and substrate analog (purple carbons) are shown as stick models. Monomer A is light teal, monomer B is dark steel blue. Helices are indicated by α1-α7 for one subunit and α1.B-α7.B for the other subunit. Beta strands similarly are β1-β4 and β1.B-β4.B. Helices 5 and 6 of each monomer form a semi-independent domain. This and most other molecular graphics images were generated using Chimera (Pettersen et al., 2004). Panels b and d of Figure 2 were created using an open source version of Pymol (DeLano, 2002). b: Structures of head-groups of FMN, NADH and nicotinic acid adenine dinucleotide (NAAD), showing ring numbering systems. In citing positions, the atom letter is followed by the position number, for example N5 in FMN. Sugar positions (not shown) are identified with a prime (').

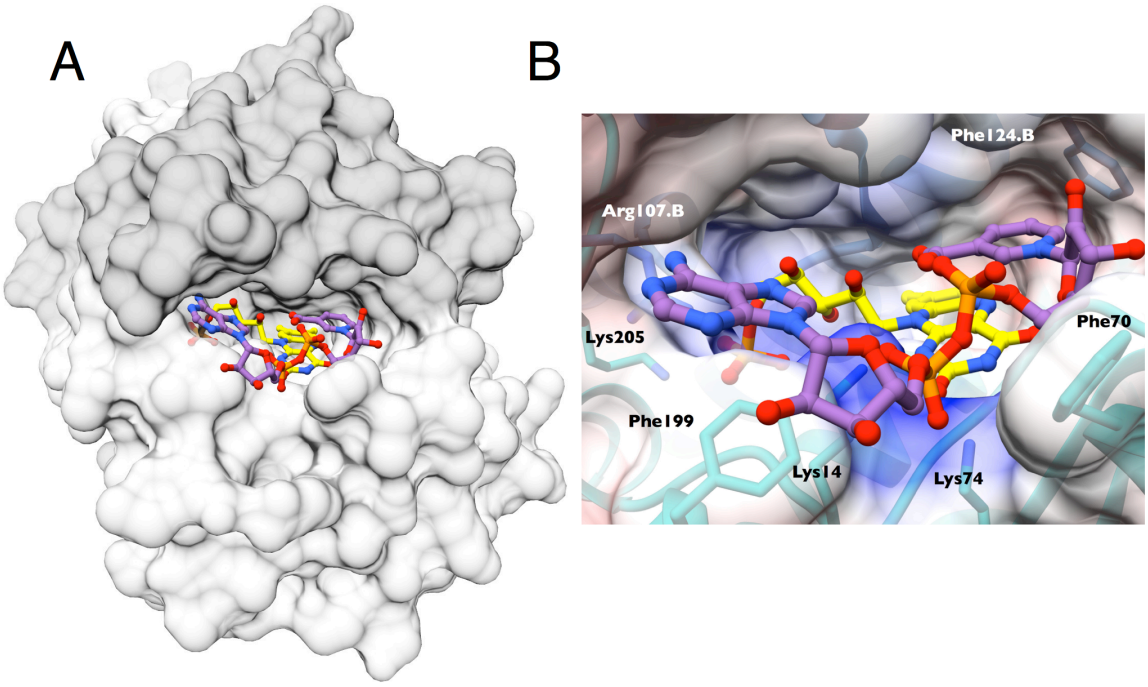

Supplemental Figure S2 related to figures 2 and 6. a: Surface view of NAAD binding to NR. NAAD (purple carbons) and flavin (yellow carbons) are shown bound to NR with dark grey surface shown for one monomer and light grey surface for the other. b: Coulomb surface representation of NR's active site with NAAD bound (stick representation with purple carbons) showing positive potential produced by protein side chains near the phosphate groups of the NAAD. Potential was calculated based on the protein only, using the Coulomb calculator in Chimera with dielectric = 4, and used to color the 1.4 Å surface from -10 (red) to +10 (blue) kcal/(mol*e^-) (Pettersen et al., 2004).

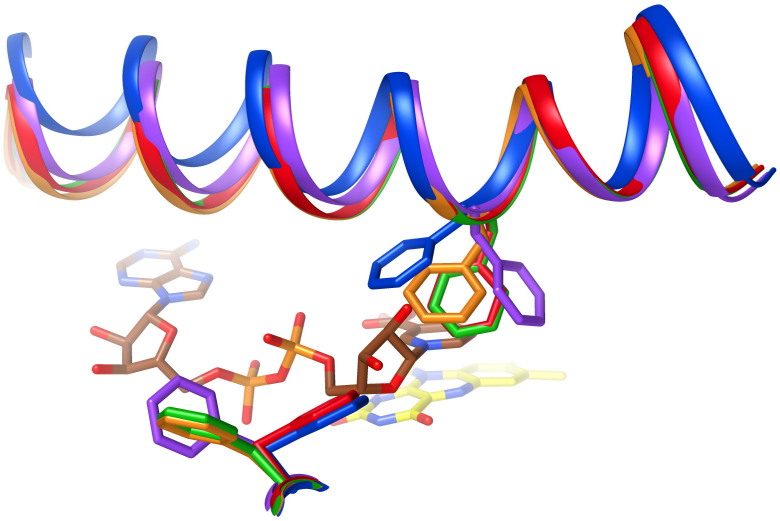

Supplemental Figure S3 related to figures 2 and 6. Comparison of the placement of Helix 6 over the active site cavities of NR•*p*-NBA (blue), NR•NAAD (purple), NR•benzoate (orange, 1KQB.pdb), NR reduced (red, 1KQD.pdb) with that of NR•acetate (green, reference structure, 1KQC.pdb). The greatest side chain movements are those of Phe70.A (below) and Phe124.A (above). The acetate, benzoate and *p*-NBA ligands are omitted for clarity but were superimposed on the nicotinamide of NAAD (compare with figure 6).

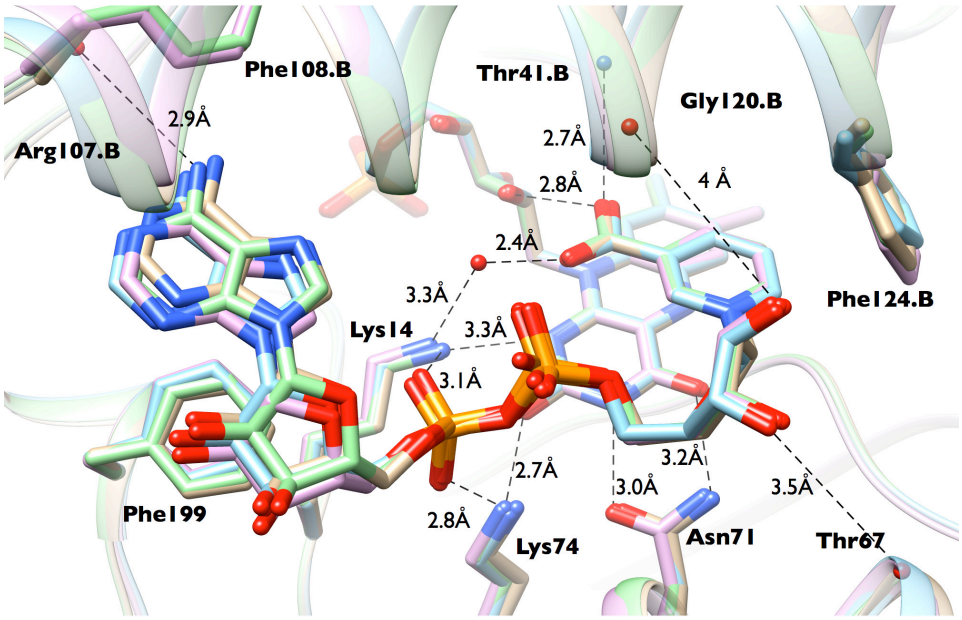

Supplemental Figure S4 related to figures 2 and 6. NAAD binding sites from each of the four crystallographically-independent active sites in the unit cell showing good superposition of the nicotinic acid moieties but a less well-defined localization of the adenine ring after superposition of the four sites using all protein atoms, in Chimera. The greater variation in the position of the adenine ring can be explained by the relative dearth of specific interactions with it compared to the nicotinic acid group. Average distances between NAAD functionalities and groups with which they interact are indicated, a water molecule is shown from one of the binding sites.

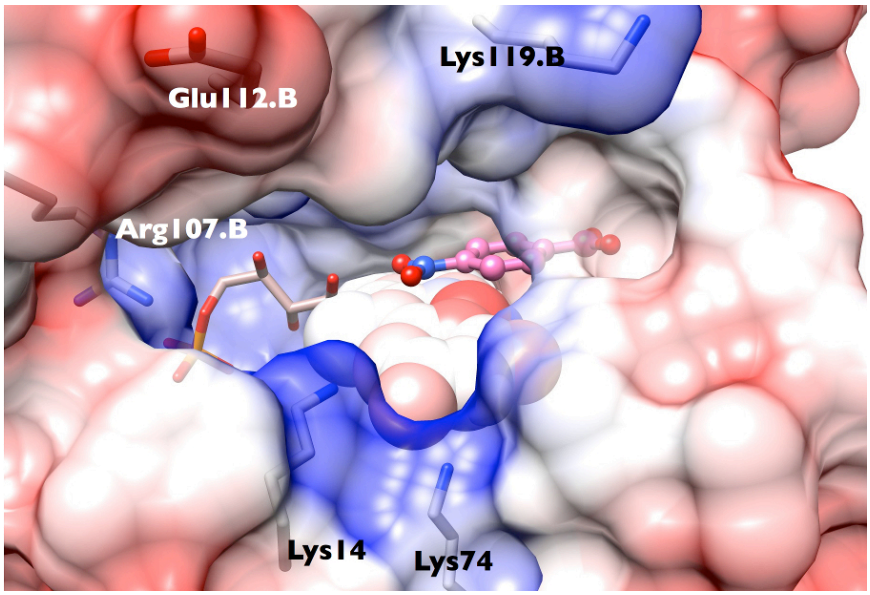

Supplemental Figure S5 related to figures 2 and 6. Change in flavin charge distribution upon reduction. Reduced anionic flavin with atoms depicted as spheres each colored by the change in NBO charge (reduced minus oxidized). NBO charges were calculated using density functional theory as implemented by Spartan for Mac (Wavefunction) using the B3LYP functional and the 6.311++G** basis set. Change in charge upon reduction (reduced - ox) is depicted with the exception of the N(5)H position which is present only in the reduced state and is colored according to its NBO charge in the reduced state. Colors range from red for a charge change of -0.35 to blue for a charge change of +0.35 and white for a charge of zero. Surface of the protein is also colored to depict the local electrostatics. The protein's H atoms were inferred using Chimera's 'add H' routine and the surface was colored from -10 (red) to +10 (blue) kcal/(mol*e^-) with dielectric = 4 and distance from surface = 1.4.

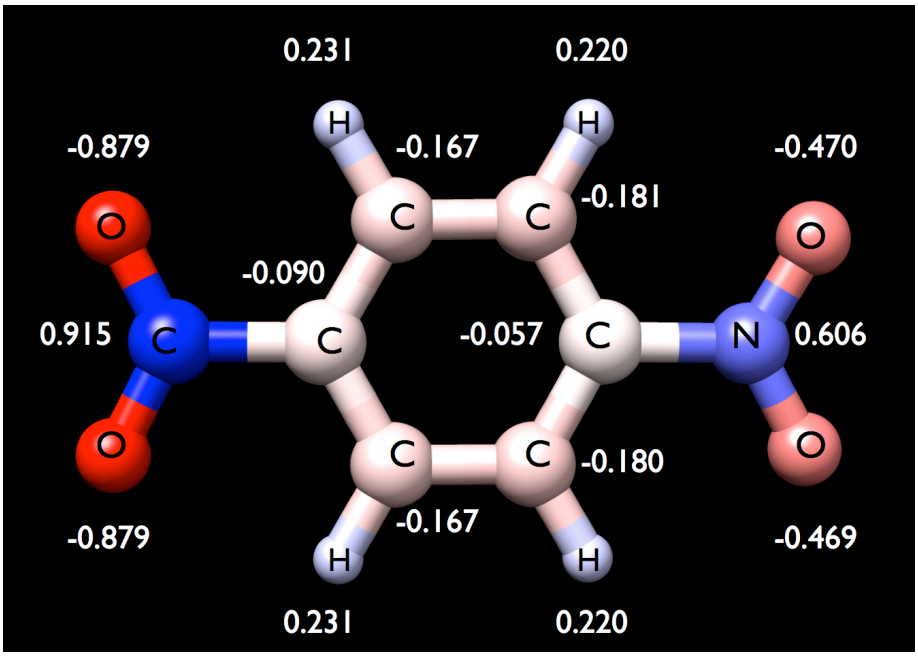

Supplemental Figure S6 related to figures 2 and 6. Natural Bond Order electron densities for *p*-NBA, computed by density functional theory calculation using the B3LYP functional and the 6.311++G** basis set as implemented by Spartan10 for Macintosh (Wavefunction.com http://wavefun.com/index.html). The position with the highest excess electron density was calculated to be the O atoms of the carboxylate (net charges of -.88) whereas the analogous O atoms of the nitro group had net charges of -.47.

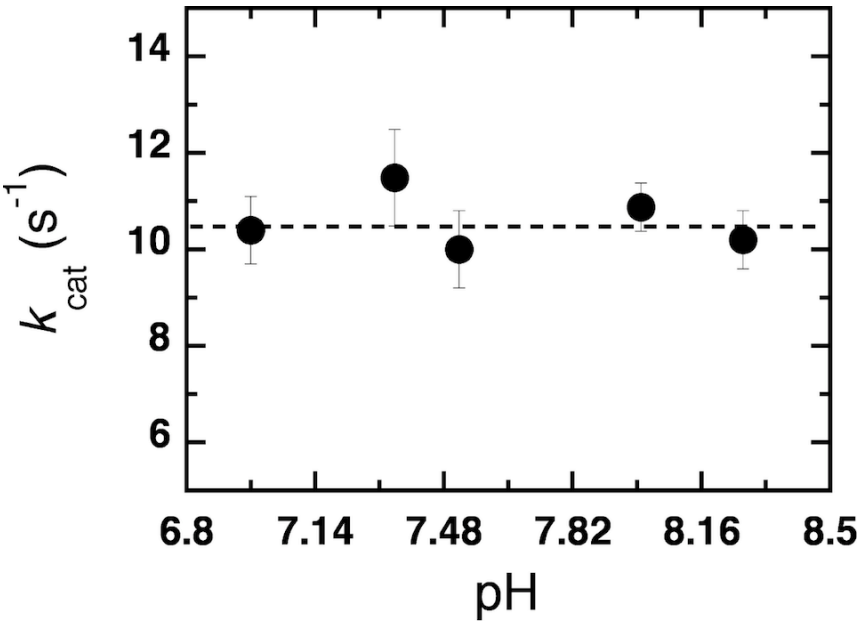

Supplemental Figure S7 related to figures 3 and 5. pH dependence of k_{cat} for NR oxidation by *p*-NBA. Initial rates were determined with 60 nM NR and various *p*-NBA concentrations (0.03, 0.06, 0.11, 0.22, 0.43, 0.52, and 0.61 mM) at a fixed NADH concentration (280 μM), pH 7.0 – 8.2, at 25 °C.

Supplemental Tables

Supplemental Table S1 related to figure 2. RMSD changes associated with binding NAAD or *p*-NBA[a]

Structure	backbone atoms	all atoms
# atoms overlayed	1728	3352
	RMSD vs. NR•acetate (Å)	
NR•NAAD.AB	0.43	0.87
NR•NAAD.CD	0.47	0.85
NR•*p*-NBA.AB (~COO proximal)	0.60 (1720 atoms)	0.90 (3336 atoms)
NR•*p*-NBA.CD (~COO proximal)	0.52	0.86
NR•*p*-NBA.AB (~NOO proximal)	0.60 (1720 atoms)	0.89 (3336 atoms)
NR•*p*-NBA.CD (~NOO proximal)	0.52	0.86

[a] Structures were overlaid on the structure of oxidized NR with acetate bound.
Each of the two crystallographic dimers were overlain in turn on the AB dimer of the acetate-bound structure using Swiss PDB viewer (Guex and Peitsch, 1997), which was also used to calculate RMSDs.

Supplemental Table S2. Interactions between NAAD, *p*-NBA, FMN and the protein related to figures 2 and 6.

Protein/Flavin contact	*p*-NBA, NOO proximal	Avg Dist (Å)	*p*-NBA, NOO distal	Avg Dist (Å)	NAAD	Avg Dist (Å)
Thr41.B NH	*p*-NBA-N**O**2'	2.8	*p*-NBA-C**O**1	2.7	Nicotinate-CO**O**	2.7
2'Ribityl-HO	*p*-NBA-N**O**2'	2.7	*p*-NBA-C**O**1	2.7	Nicotinate-CO**O**	2.8
(H_2O)[a]	*p*-NBA-N**O**2'	5[a]				2.4[a]
Phe124.B Ar	*p*-NBA Ar	3.7	*p*-NBA Ar	3.6	Nicotinate Ar	3.7[b]
H_2O	*p*-NBA-C**O**1	2.6[b]	*p*-NBA-N**O**2	2.7[a,b]		
His128.B-**N**E2	H_2**O**	3.0[b]	H_2**O**	2.7[a,b]		
Glu165-CO**O**	H_2**O**	2.7	H_2**O**	2.9		
FMN N5	pNBA-**N**OO	4.0	*p*-NBA-**N**OO	5.4	Nicotinate **C4**	**3.0**
FMN N5	pNBA-**C**OO	5.5	*p*-NBA-**C**OO	3.9		
FMN N5	*p*-NBA-NO2' (inward-facing)	**3.9**	*p*-NBA-CO1 (inward-facing)	3.9		
FMN N5	*p*-NBA-NO1' (outward-facing)	4.8	*p*-NBA-CO2 (outward-facing)	4.9		
FMN N5	*p*-NBA-CO1 (inward-facing)	5.6	*p*-NBA-NO2' (inward-facing)	**5.6**		
FMN N5	*p*-NBA-CO2 (outward-facing)	6.3	*p*-NBA-NO1' (outward-facing)	6.3		
Gly120.B **O**					N-ribose **O**2'	4.2
Thr67 **O**					N-ribose **O**3'	3.5[b]
Asn71-CO**N**H_2					N-ribose **O**4'	3.0
Lys14-**N**H_3					A-P$O4^-$ **O**2	3.1
Lys74-**N**H_3					A-P$O4^-$ **O**1	2.8
Phe108.B Ar					Adenine **N**H_2	3.6[b]
Arg107.B **O**					Adenine **N**H_2	2.9[b]
Phe199 Ar					Adenine Ar	3.7
FMN N5	Glu165 N	3.1		3.1		3.2
FMN O4	Glu165 N	3.3		3.4		3.4
FMN O4	Gly166 N	3.0		3.1		2.9
FMN O4	Asn71-CO**N**H_2	3.2		3.1		3.0
FMN N3	Asn71-C**O**NH_2	3.1		3.0		3.0
FMN O2	Lys74-**N**H_3	2.8		2.8		2.7
FMN O2	Lys14-**N**H_3	2.6		2.6		2.6
FMN N1	Lys 14-**N**H_3	3.3		3.3		3.3

[a] The crystallographic waters vary in occupancy and position among the 4 active sites.
[b] standard deviation among the distances measured in the four active sites exceeded 5% of the average distance.